«ФИЗИКА ЭЛЕМЕНТАРНЫХ ЧАСТИЦ И АТОМНОГО ЯДРА»
2000, ТОМ 31, ВЫП. 7А

УДК 539.14

# STRUCTURE OF NUCLEONS

*I.A.Savin*

Joint Institute for Nuclear Research, 141980, Dubna, Russia

The experimental data confirming the quark structure of the nucleons are reviewed with the emphasis on the experiments with JINR participation.

## 1. INTRODUCTION

The experimental studies of the nucleon structure have been initiated at JINR by N.N.Bogoliubov. In 1974, he has assigned a group of JINR physicists to join one of the CERN collaboration and propose a common CERN–JINR experiment in this field. A Proposal to study the nucleon structure in Deep Inelastic Scattering (DIS) of muons on protons, deuterons and heavy targets in the wide kinematic region up to the highest accessible four-momentum transfer at CERN–SPS has been prepared by the Bologna–CERN–Dubna–Munich–Saclay (BCDMS) Collaboration same year and approved in 1975 as the NA-4 experiment to run from 1979. The results [1] of the BCDMS Collaboration on the proton structure function, $F_2^p(x,Q^2)$, and on the nucleon structure functions $F_2^D(x,Q^2)$ and $F_2^C(x,Q^2)$ measured with deuterium and carbon targets as well as nuclear effects in the ratios of structure functions measured simultaneously with carbon and deuterium $F_2^C(x,Q^2)/F_2^D(x,Q^2)$, or nitrogen and deuterium targets, $F_2^N(x,Q^2)/F_2^D(x,Q^2)$, are ones of the most precise in the studied kinematic range.

Since the BCDMS experiment at CERN (1975–1985), JINR participates in a series of the nucleon structure experiments, particularly in the experiment of the Spin Muon Collaboration (SMC) at CERN [2] with longitudinally polarized muons and longitudinally and transversely polarized protons and deuterons (1985–1998), in the HERMES experiment at DESY [3] using the polarized electrons of the HERA collider and internal polarized and unpolarized gas targets (since 1994), in the experiments under preparations with the STAR Detector at RHIC, BNL [4] using relativistic ions and polarized proton beams (since 1995) and COMPASS at CERN (since 1998) [5].

In this talk I would like to give a general overview of the subject to which N.N.Bogoliubov has made an important contribution suggesting a concept of a color [6].

As is well known, the nucleon structure is probed in the inclusive reactions of the lepton-nucleon ($l$N) DIS. These reactions are mediated by a virtual photon or/and Z boson exchange. At present energies of fixed target experiments, the main contribution to the charged lepton DIS cross sections (which are the main subjects of the talk) comes from the one-photon exchange process although the interference between the photon and Z exchange ($\gamma$Z interference) is observed in eN and $\mu$N reactions.

The theoretical expressions for the unpolarized $l^{\pm}N$ cross sections contain the phenomenological structure functions $F_1(x, Q^2)$ and $F_2(x, Q^2)$ and additionally two structure functions $g_1(x, Q^2)$ and $g_2(x, Q^2)$ in case of polarized particles (the standard DIS notations are used here). The physical interpretation of these structure functions one can obtain only in the framework of particular models of the nucleon structure [7].

## 2. UNPOLARIZED STRUCTURE FUNCTIONS AND THEIR INTERPRETATION

A number of DIS experiments have been performed up to now in various lepton beams. The most precise of them are

— eN experiments at SLAC by several collaborations and at DESY by the HERMES, H1 and ZEUS collaborations;

— $\mu$N experiments at CERN by the EMC, BCDMS, NMC and SMC and at FNAL by the E665 collaborations;

— $\nu$N experiments at CERN by the CDHS and CHARM and at FNAL by the CCFR collaborations.

Starting from the BCDMS experiment the «standard» requirement for the precision DIS experiment is about 1–2 %. The representative data [8] on structure functions $F_2(x, Q^2)$ are shown in Fig.1. The data cover the kinematical region from 1 to 1000 GeV$^2$ in $Q^2$ and from $10^{-4}$ to 1 in $x$. One can see a remarkable agreement between the data obtained by different experiments. The most precise data on $F_2(x, Q^2)$ for the proton and deuterium are obtained by the charged-lepton experiments.

The data on $F_2$ are interpreted most fruitfully in terms of nucleon structure using the Quark-Parton Model (QPM).

According to QPM nucleons consist of pointlike partons associated with quarks and gluons. In more detail nucleons contain three valence quarks bound by gluon exchange and a sea of quark-antiquark pairs of different flavors emitted by gluons.

In the so-called «naive» QPM the variable $x$ (Bjorken variable) takes the simple meaning of a fraction of the nucleon three-momentum carried by the quark which has been struck in the interaction with virtual photon. This interpretation

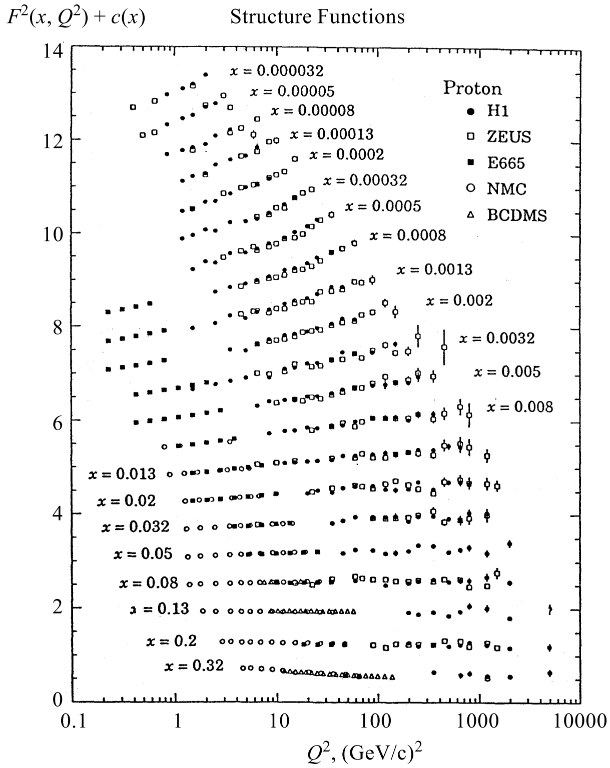


Fig. 1. The representative world data on the proton structure function $F_2^p(x, Q^2)$ shown as a function of $Q^2$ for different $x$ bins

is valid only in the Breit frame, or infinite momentum frame, where quark masses and transverse momenta are neglected. In the same reference frame, assuming that quarks are pointlike particles, the structure functions should depend on a single dimensionless variable $x$ only (the Bjorken scaling hypothesis) and can be represented as linear combinations of quark distribution functions $q(x)$:

$$F_1^l(x) = \frac{1}{2} \sum_i e_i^2 [q_i(x) + \bar{q}_i(x)], \tag{1}$$

$$F_2^l(x) = x \sum_i e_i^2 [q_i(x) + \bar{q}_i(x)], \tag{2}$$

where the $e_i$ are the electric charges of the quarks and the index $i$ runs over all quark flavors. For the most of the fixed target experiments on DIS there are four active quarks contributing to the $F_2$: up ($u$), down ($d$), strange ($s$) and charm ($c$) quarks.

Expressions for the structure functions $F_i^l$ measured with charged leptons contain square of quark charges. This is due to electromagnetic interaction which is proportional to $e^2$. The expressions similar to (1) and (2) can be obtained within QPM for interactions mediated by weak interactions which do not depend on electric charges:

$$F_1^{\nu}(x) = \frac{1}{2}\sum[q_i(x) + \bar{q}_i(x)], \tag{3}$$

$$F_2^{\nu}(x) = x\sum[q_i(x) + \bar{q}_i(x)], \tag{4}$$

$$xF_3^{\nu}(x) = \sum[q_i(x) - \bar{q}_i(x)]. \tag{5}$$

The third structure function $xF_3^{\nu}$ has appeared due to a $V-A$ nature of weak interactions.

At finite energies the structure functions should depend on two variables, and the simple relationship between $F_1$ and $F_2$ known as the Callas–Gross theorem, $F_2(x) = 2xF_1(x)$, is replaced by the relation introducing the so-called longitudinal structure function

$$F_L(x, Q^2) = F_2(x, Q^2)\left[1 + \frac{4M^2x}{Q^2}\right] - 2F_1(x, Q^2) \tag{6}$$

which is in turn related to the ratio of absorption cross section for longitudinally and transversely polarized virtual photons

$$R = \frac{\sigma_L}{\sigma_T} = \frac{F_L}{2xF_1}. \tag{7}$$

The results of DIS experiments are published most commonly in terms of structure functions $F_2$ and $R$. The set of these measurements is used for various interpretations and comparison with models.

The shapes of structure functions measured in different beams were used to check the basic assumption of QPM of nucleons. Particularly from Exps.(2) and (4) follows that the structure functions $F_2^l$ and $F_2^{\nu}$ should be identical up to the normalization factor $\approx 5/18$. This has been successfully proved by CERN neutrino and muon experiments.

A number of sum rules for structure functions and their ratios are used to determine the number of valence quarks in the proton, quark charges, total momentum carried by quarks, etc.

One of the most important results of DIS experiments was the observation of the scaling violation in structure functions. As one can see from data on $F_2$ the scaling hypothesis is approximately valid only in the narrow region of $x$ around $x \approx 0.2$. At other $x$ the scaling is violated:

— at $x < 0.2$ $F_2$ is increased with increasing $Q^2$,

— at $x > 0.2$ $F_2$ is decreased with increasing $Q^2$.

Such a pattern is explained by Quantum Chromodynamics (QCD).

As is known, the main assumption of QCD is that the strong interaction coupling $\alpha_s(Q^2)$ depends on $Q^2$. This dependence is controlled by the renormalization equation with beta functions $\beta_i$, $i = 0, 1, 2,...$:

$$\mu\frac{d\alpha_s}{d\mu} = -\frac{\beta_0}{2\pi}\alpha_s^3 - \frac{\beta_1}{4\pi^2}\alpha_s^3 - \frac{\beta_2}{64\pi^3}\alpha_s^4 ... \tag{8}$$

where $\beta_0 = 11 - \frac{2}{3}N_f$ for the Leading Order (LO),
$\beta_1 = 102 - \frac{38}{3}N_f$ for the Next-to-Leading Order (NLO),
$\beta_2 = 2857 - \frac{5033}{9}N_f \frac{325}{27}N_f$ for the Next-to NLO

and $N_f$ is a number of active flavors.

The solution of the renormalization equation truncated to NLO gives

$$\alpha_s(Q^2) = \frac{4\pi}{\beta_0 ln(Q^2/\Lambda^2)}\left[1 - \frac{\beta_1}{\beta_0}\cdot\frac{lnln(Q^2/\Lambda^2)}{ln(Q^2/\Lambda^2)}\right], \tag{9}$$

where $\Lambda$ is the mass scale of QCD. It is not predicted by QCD itself and can only be determined by experiments.

Since $\alpha_s(Q^2)$ is a physical observable, the numerical value of $\Lambda$ depends on $N_f$ and, beyond of LO, on the renormalization scheme used to compute the perturbative QCD expansion. Usually the so-called «Modified minimal subtraction» scheme is used and corresponding $\Lambda$ is $\Lambda\frac{N_f}{MS}$.

QCD predicts a $Q^2$ evolution of the nonsinglet (NS) and singlet (SI) in a flavor space quark distributions which are proportional to the difference and sum of quark distribution functions, respectively:

$$q^{NS} \sim q(x) - \bar{q}(x), \quad q^{SI} \sim q(x) + \bar{q}(x).$$

Any structure function can be decomposed into a linear combination of these and gluon distributions.

Technically the QCD predictions for structure functions are compared to the data using three methods:

1. Evolution equations for the nonsinglet, singlet and gluon distributions;
2. Evolution of moments of structure functions;
3. Dependence on $x$ of the logarithmic derivatives (slopes) of structure functions.

Predictions 1 and 2 require a knowledge of parton distributions at a boundary $Q^2 = Q_0^2$. It is not predicted by QCD and should be found from an experiment.

The QCD methods of analysis of DIS data were developed in parallel with increasing of the data precision. At the beginning of the BCDMS experiments the practical procedures of QCD tests were developed only for the first method up to NLO NS and to LO for SI distributions. The BCDMS has developed and applied all three methods up to NLO for SI and NS structure functions. The second method has been developed at JINR in an original form expanding the structure functions in a series of Jacobi polynomials and moments [9].

Analyzing the own precision data in the region $x = 0.07 \div 0.8$ and $Q^2 = 10 - 260$ GeV$^2$ BCDMS has obtained a full agreement with QCD using all three above methods. Particularly, BCDMS has shown that the NLO approximation is very important for the correct description of the data by QCD.

Results of the QCD analysis performed by other experiments before BCDMS were controversial [10]. Reanalyzing these data, BCDMS has demonstrated that in some cases analysis was incomplete, i.e., in LO approximation only, in other cases data were contaminated by non-QCD processes, either by background, or by the so-called higher twist (HT) contributions. Assuming that HT contribute in a form

$$F_2(x, Q^2) = F_2^{QCD}(x, Q^2)[1 + C_{HT}(x)/Q^2]. \quad (10)$$

BCDMS has extended the agreement of the combined SLAC and BCDMS data up to $Q^2 = 1$ GeV$^2$ (see Fig.2). For the combined data: $\Lambda_{\overline{MS}}^{(4)} = 263 \pm 42$ MeV corresponding to $\alpha_s(M_z^2)$

$$\alpha_s(M_z^2) = 0.113 \pm 0.003(\mathrm{exp}) \pm 0.004(\mathrm{th}),$$

where experimental errors include both statistical and systematic uncertainties. This is one of the most precise determination of $\alpha_s(M_z^2)$ dominating the present world average value:

$$\alpha_s(M_z^2)_{w.av.} = 0.118 \pm 0.002(\mathrm{exp}) \pm 0.004(\mathrm{th}).$$

As one can see, the theoretical errors are larger than the experimental ones. Further progress in theory is needed to reduce these uncertainties.

## 3. POLARIZED STRUCTURE FUNCTIONS AND THEIR INTERPRETATION

The phenomenology of polarized DIS reactions one can find in [11] and references therein. As is shown there, the spin-dependent structure functions $g_1^p$, $g_1^d$ and $g_2^p$, $g_2^d$ of the proton and deuteron are expressed via experimentally measured cross section asymmetries $A_{II}^{p,d}$ and $A_{\perp}^{p,d}$.

$$A_{II}^{p,d} = \frac{\sigma_{\uparrow\downarrow} - \sigma_{\uparrow\downarrow}^{p,d}}{\sigma_{\uparrow\downarrow}^{p,d}}; \quad A_{\perp}^{p,d} = \frac{\sigma_{\uparrow\rightarrow}^{p,d} - \sigma_{\uparrow\leftarrow}^{p,d}}{\sigma_{\uparrow\rightarrow}^{p,d} + \sigma_{\uparrow\leftarrow}^{p,d}}. \quad (11)$$

The asymmetry $A_{II}(A_{\perp})$ is measured with the longitudinally polarized beam and longitudinally (transversely) polarized target.

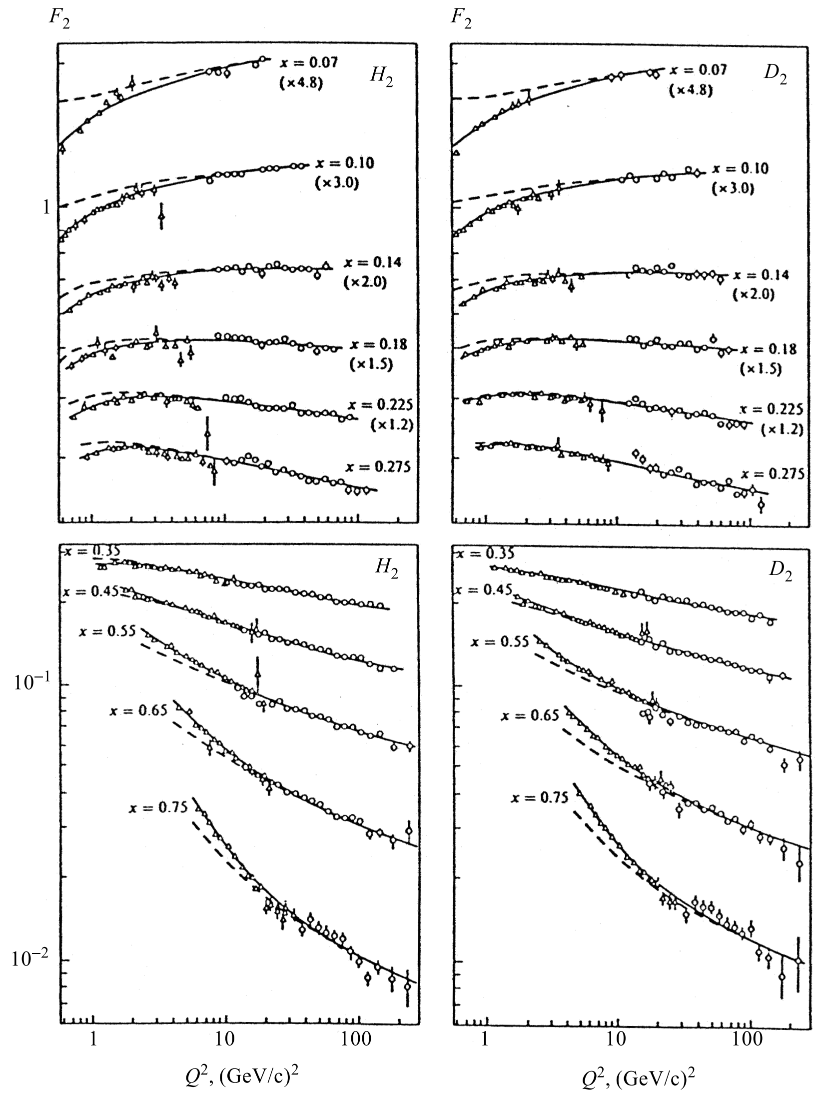


Fig. 2. Results of the QCD analysis of the combined BCDMS and SLAC data on the $F_2^p(x, Q^2)$. The dashed lines show purely perturbative fits. The solid lines include also higher twist contributions

The asymmetries $A_{II}$ and $A_\perp$ in the one-photon exchange approximation are related to the virtual photon asymmetries $A_1$ and $A_2$ and structure functions $g_1$ and $g_2$.

To the first approximation

$$A_{II}^{p,d} \approx D A_1^{p,d}; \quad A_{\perp}^{p,d} \approx d A_2^{p,d} \tag{12}$$

and

$$g_1^{p,d} \approx \frac{F^{p,d}}{2x(1+R)} \cdot \frac{A_{II}^{p,d}}{D}; \quad g_2^{p,d} \approx \frac{F^{p,d}}{2x(1+R)} \cdot \frac{A_{\perp}^{p,d}}{d\gamma}, \tag{13}$$

where $\gamma$ is kinematical factor, $D$ and $d$ are virtual photon depolarization factors.

The structure function $g_1$ is an object of the special interest to spin physics because in the QPM it can be interpreted as a difference of two probabilities, $q_i^{\uparrow}(x)$ and $q_i^{\downarrow}(x)$, averaged over the quark flavor charges:

$$g_1(x) = \sum_i e_i^2 \left[ q_i^{\uparrow}(x) - q_i^{\downarrow}(x) \right] \equiv \sum_i e_i^2 \Delta q_i^{\uparrow\downarrow}(x). \tag{14}$$

Here $q_i^{\uparrow}(x)$, $(q_i^{\downarrow}(x))$ is a probability that in a longitudinally polarized nucleon the quark $i$ has a fraction $x$ of the nucleon momentum and a spin aligned along (opposite to) the nucleon spin. To some extent, $g_1(x)$ characterizes a partial contribution of quarks to the nucleon spin.

The $g_1$ is also interesting for measurements aiming to test the famous Bjorken and Ellis–Jaffe sum rules. These sum rules involve the first moments of the structure function $g_1$, $\Gamma_1$:

$$\Gamma_1^{p,n,d} = \int_0^1 g_1^{p,n,d}(x) dx. \tag{15}$$

In QPM the $\Gamma_1$ represents a total contribution of active quark flavors to the nucleon spin.

The Bjorken sum rule for $\Gamma^p - \Gamma^n$ has been derived for the first time about 30 years ago in asymptotic limit $Q^2 \to \infty$ using the quark current algebra and assuming standard quark charge assignment and isospin symmetry for quark distributions in nucleons:

$$\Gamma_1^p - \Gamma_1^n = \int_0^1 \left[ g_1^p(x) - g_1^n(x) \right] dx = \frac{1}{6} \left| \frac{g_A}{g_V} \right|, \tag{16}$$

where $g_A(g_V)$ is an axial (vector) coupling constant of weak interactions. Now the Bjorken sum rule is derived in QCD, i.e., the $\Gamma_1^p - \Gamma_1^n$ is $Q^2$-dependent. The Bjorken sum rule is independent of nucleon spin structure details and due to that is of the fundamental importance for the present understanding of elementary particles.

The Ellis–Jaffe sum rules for $\Gamma_1^p$ and $\Gamma_1^n$ have been derived using the same, as for the Bjorken, sum rule assumptions and additionally assuming the SU(3) symmetry in decays of the octet baryons and zero net polarization for strange sea quarks in nucleons:

$$\Gamma_1^{p(n)} = \int_0^1 g_1^{p(n)}(x)dx = \frac{1}{12}\left|\frac{g_A}{g_V}\right|\left(\substack{+\\(-)}1 + \frac{5}{3}\cdot\frac{3\frac{F}{D}-1}{\frac{F}{D}+1}\right), \qquad (17)$$

where $F$ and $D$ are SU(3) couplings describing the $\beta$-decays of the baryon octet members. In QCD, the Ellis–Jaffe sum rules are the subject of corrections calculated now up to the second order in $\alpha_s(Q^2)$.

The first measurement of the $g_1^p(x)$ has been performed by SLAC experiments E80 and E130 and published in 1980. The kinematic range of these measurements was $x = 0.1 \div 0.7$. Nothing unexpected has been seen either for $A_1^p(x)$ or for $g_1^p(x)$. Surprises came later, when in 1988 the European Muon Collaboration (EMC) at CERN has repeated the measurements of $g_1^p$ in the extended $x$ range from 0.01 to 0.7 and found that $\Gamma_1^p$ is less than the Ellis–Jaffe prediction by about three standard deviations. From the measured $\Gamma_1^p$ the EMC has found that quarks contribute little to the proton spin and strange quark sea is probably polarized negatively. The EMC results have originated the so-called spin crisis which became the subject of many experimental and theoretical works. New experiments have been suggested in 1989: SMC at CERN, E142 and E143 at SLAC, HERMES at DESY and later on E154 and E155 at SLAC.

The SMC experiment has been approved to start data taking in 1991.The goals of the SMC were

— to confirm the first SLAC/EMC measurements on $g_1^p$ with improved accuracy,
— to obtain new data on $g_1^d$ and, as a consequence, on $g_1^n$,
— to measure the second spin-dependent structure function $g_2^{p,d}$ for the first time,
— to test the Bjorken sum rule for the first time.

The final SMC data and other available data on $g_1$ [2,8] are presented in Fig.3. The corresponding values of the moments corrected for unmeasured $x$ regions and calculated at $Q_0^2 = 10$ GeV$^2$ are given below. They differ from the Ellis–Jaffe predictions by several standard deviations:

| SMC | ELLIS–JAFFE | |
|---|---|---|
| $\Gamma_1^p(Q_0^2) = 0.120 \pm 0.005(\mathrm{st}) \pm 0.006(\mathrm{syst}) \pm 0.014(\mathrm{th})$, | $0.176 \pm 0.004$, | (18) |
| $\Gamma_1^d(Q_0^2) = 0.019 \pm 0.006 \pm 0.003 \pm 0.013$, | $0.068 \pm 0.004$. | (19) |

Note, that the largest contributions to the errors come from theoretical uncertainties which have been underestimated in earlier publications.

Knowing the $g_1^p$ and $g_2^d$, one can calculate a nonsinglet structure function $g_1^{NS}(x, Q_2) = g_1^p - g_1^n$ and its moment $\Gamma_1^{NS}$ confirming the Bjorken sum rule:

| SMC | Bjorken |
|---|---|
| $\Gamma_1^{NS}(Q_1^2)$=0.198±0.023 | 0.186±0.03. |

The SMC has performed the most complete NLO QCD fits to the world data on $g_1(x, Q^2)$. The results at $Q_0^2 =$ 5 GeV$^2$ are presented in Fig.4. The data points are shown with statistical errors only. The estimations of experimental systematic and theoretical uncertainties are given separately by vertically and horizontally hatched bands, respectively. One can comment these results as following:

— there is an agreement between the data and fitted curves (solid lines);

— negative values of $g_1^p(x)$ are predicted by present QCD analysis for $x \leq 10^{-3}$;

— the errors of all measurements are still too big to make quantitative conclusions.

The data are in good agreement with QCD. The strong interaction constant determined from this analysis, $\alpha_s(M_z^2) = 0.121 \pm 0.006$, coincides with the world average determined from other experiments.

Using the results of the QCD analysis of the world data on $g_1$, one can calculate the first moments of the $g_1$ and test the Bjorken sum rule:

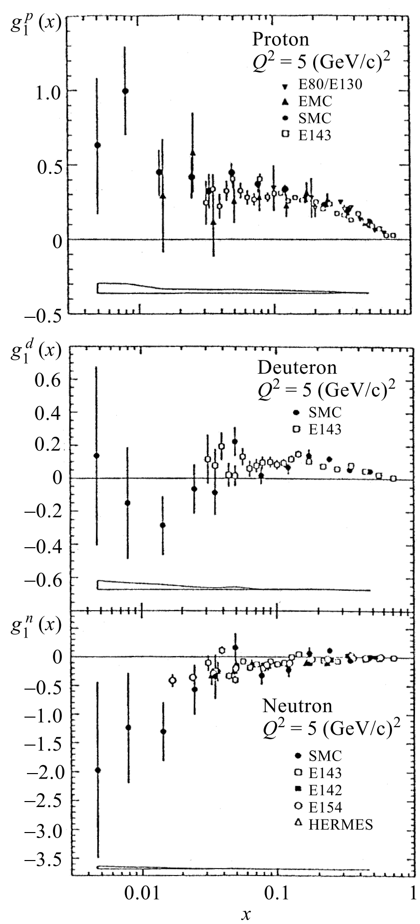


Fig. 3. The world data on the spin-dependent structure function $g_1(x)$ of the proton, deuterium and neutron envolved to the common value of $Q^2 = 5$ GeV$^2$

| | World data | Theory |
|---|---|---|
| $\Gamma_1^p - \Gamma_1^n$ at $Q^2 = 5$ GeV$^2$ | $0.173^{+0.024}_{-0.012}$ | $0.181 \pm 0.003.$ |

As is seen, the rule is confirmed within the errors.

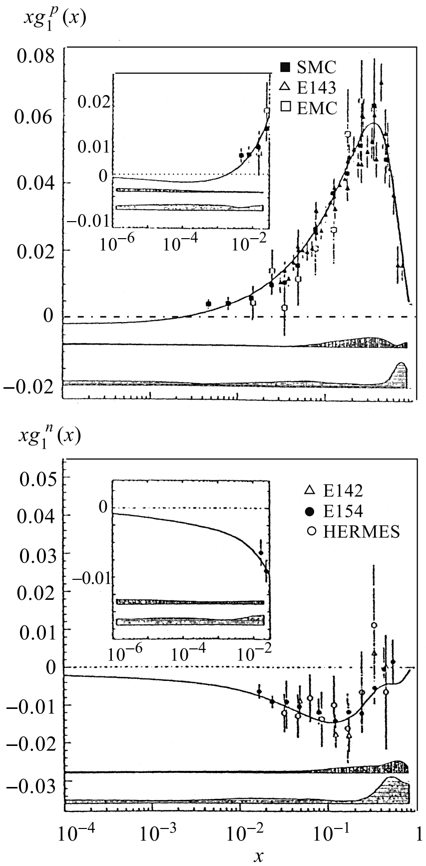


Fig. 4. The result of the QCD fits of the world data on the $g_1(x, Q^2)$ shown at the common $Q^2 = 5$ GeV$^2$

From the same analysis one can calculate also the first moments of the gluon, $\Delta G(Q^2)$, and singlet quark, $\Delta\Sigma(Q^2)$, distributions which represent the total gluon and quark contributions to the spin of nucleons, respectively. It was found at $Q^2 = 1$ GeV$^2$ that

$$\Delta\Sigma(Q^2) = 0.23 \pm 0.07 \pm 0.16$$

and

$$\Delta G(Q^2) = 0.99^{+1.17+0.42+1.43}_{-0.31-0.22-0.45}.$$

So, the present world data confirm the original EMC result on the small contribution of quarks to the spin of proton. Unfortunately the present data on $g_1$ are not precise enough to determine $\Delta G$. Dedicated experiments for $\Delta G$ measurements are planned by the HERMES, COMPASS and STAR collaborations.

## 4. NUCLEAR EFFECTS IN STRUCTURE FUNCTION

Because the DIS cross sections at large $Q^2$ are small, earlier DIS experiments have used heavy nuclei to increase statistics by a factor $A$, where $A$ is an atomic number of the target. This has been motivated by a fact that in DIS reactions a momentum transfer to the bound nucleon is of the order $k \sim \sqrt{Q^2} \approx 1 - 10$ GeV, i.e., three orders of magnitude larger than nucleon binding. So, for DIS one can assume that nucleons in nuclei are «free». Possible violation of this assumption one could expect at very small ($x \ll 0.1$) or at very large $x$ ($x \geq 0.8$), where effects of nucleon (anti)shadowing and Fermi motion can play role, respectively. It was generally assumed that at $0.05 < x < 0.8$:

$$A \cdot F_i^A(x, Q^2) = zF_i^p(x, Q^2) + (A - Z)F_i^n(x, Q^2),$$

or at $A = 2Z$:

$$F_i^A(x, Q^2) = A/2 \cdot F_i^D(x, Q^2), \quad F_i^D(x, Q^2) = \frac{1}{2}(F_i^p + F_i^n).$$

.

For the last case the ratio $r^A = F_2^A(x, Q^2)/F_2^D(x, Q^2)$ is expected to be close to unity. But unexpectedly the EMC has found in 1983 that the ratios $r^{\mathrm{Fe}}(x)$ are $x$-dependent and substantially differ from 1 in the region of $x = 0.1 \div 0.7$ although the experimental errors were large. This so-called «EMC effect» has been interpreted in a sense that the structure of the bound nucleons is different from that of free nucleons. Such a statement required further precision studies and theoretical understanding.

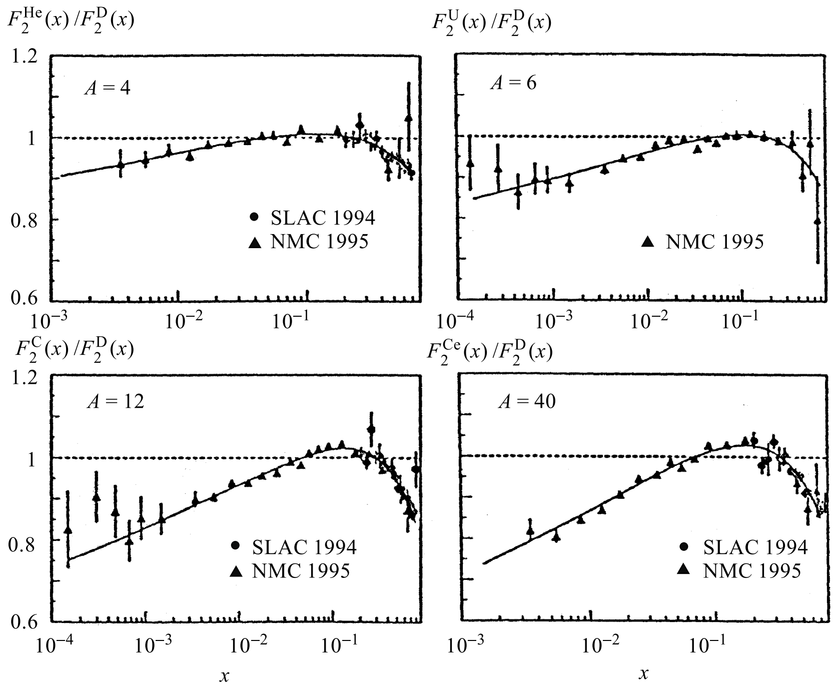


Fig. 5. The results of the phenomenological fit of structure function ratios $F_2^A/F_2^D$ measured by the NMC and SLAC collaborations in the range $x = 0.0001 \div 0.7$

Further precision studies of the nuclear effects in structure functions performed in 1984-1992 by SLAC-E139, BCDMS, EMC-NA2, EMC-NA28, NMC and FNAL E665 have confirmed the EMC effect at $x = 0.3 \div 0.7$, corrected its absolute value and $x$-dependence at $x < 0.3$, observed minimum in $r^A(x)$ at $x = 0.65$, shadowing–antishadowing at $x < 0.1$, weak $A$ dependence and no $Q^2$

dependence. Combining all experimental observations, one could see [12] that $r^A(x)$ has an oscillating shape with three $A$-independent cross over points where $r^A(x_i) = 1$ $i = 1, 2, 3$. The cross over point $x_1 \approx 0.1$ separates the effects of shadowing and antishadowing, $x_2 \approx 0.3$ separates effects of antishadowing and EMC and $x_3 \approx 0.8$ separates effects of EMC and Fermi motion. There is no unique theoretical model describing all these effects. Some models explain part of the data [13]. In the phenomenological analysis [14] a simple parametrization of all data on $r^A(x)$ is found (see Fig. 5) and two-stage concept of the distortion of quark distributions in bound nucleons is suggested. At the first stage the distortion is a function of $x$ and $A$ for $A \leq 4$ and at the second stage at $A > 4$ the distortion evolves as a function of $A$ only. This evolution is proportional to the evolution of the nucleon density at the nuclear surface given by the Woods–Saxon potential.

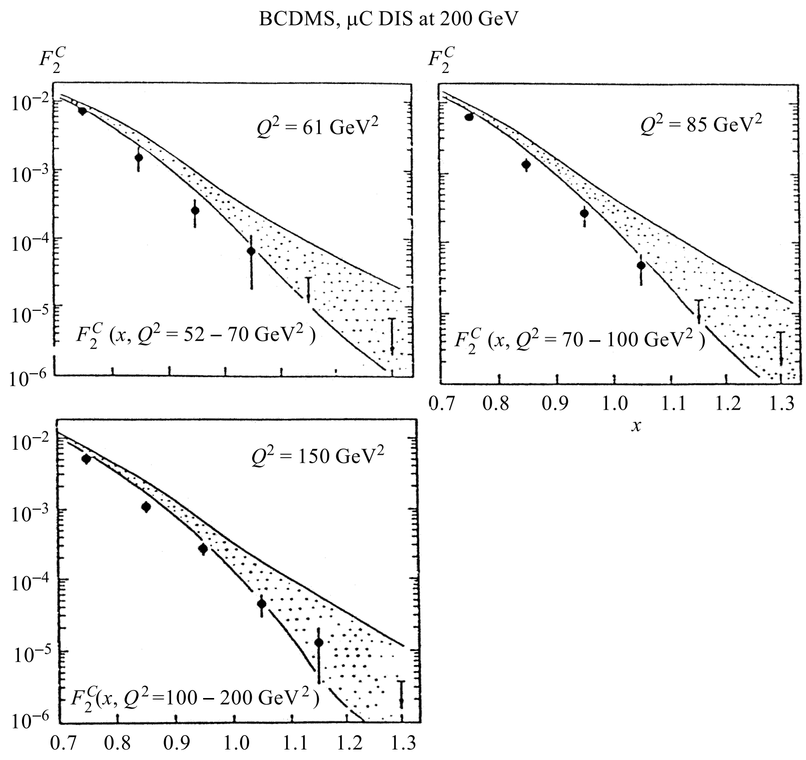


Fig. 6. Nucleon structure function $F_2^C$ as a function of $x$ at three values of $Q^2$. The hatched areas correspond to the Frankfurt and Strikman predictions

Another manifestation of nuclear effects in structure functions would be on observation of $F_2^A$ at $x > 1$. For a free nucleon the value $x = 1$ is a kinematical limit and $F_2(x \geq 1) = 0$. For a bound nucleon $F_2^A(x \geq 1) > 0$ due to its Fermi motion in nuclei or possible existence in a nuclei of the nucleon (quark) clusters. The only available BCDMS data [12] on the $x$-dependence of the nucleon structure function in carbon, $F_2^C(x)$, at large $x$ up to $x = 1.2$ have shown (see Fig.6) that such clusters indeed could exist.

## 5. CONCLUSIONS

In conclusion one can give a list of DIS discoveries confirming the QPM of nucleons:

1. Nucleons consist of quarks and gluons.
2. Quarks are pointlike particles.
3. Quarks have a spin $1/2$.
4. Quarks have fractional charges $1/3$ and $2/3$.
5. Nucleons contain 3 valence quarks: $\mathrm{p} = u_v u_v d_v$, $\mathrm{n} = d_v d_v u_v$. Quarks $u_v$ and $d_v$ have different $x$ distributions.
6. Nucleons have a sea of quark–antiquark pairs — sea quarks picked at small $x$.
7. Quarks carry about 50 % of the total nucleon momentum, about the same is carried by gluons.
8. Scaling hypothesis of the structure function behavior is violated. The violation is the same in eN, $\mu$N and $\nu$N DIS. It is explained in QCD improved QPM.
9. The fundamental Bjorken sum rule for polarized structure functions is confirmed. The Ellis–Jaffe sum rules are violated. The contributions of quarks to the spin of nucleons are determined. The total contribution of quarks to the spin is found to be about 30 %.
10. Electroweak interference in eN and $\mu$N DIS is observed confirming the Standard Model expectations.
11. Nuclear effects including the EMC effect are observed in structure functions of the nucleons bound in nuclei. The nuclear environment distorts the $x$ distributions of bound nucleons compared to that of free nucleons, etc. These and other observations require a deep theoretical understanding.

Finally, one can mention that DIS and the nucleon structure were the subjects of all large scale International Conferences for last 30 years. The subject is still very actual. The characteristic features of the next-generation DIS experiments are semiinclusive and exclusive reactions pointing to specific problems of polarized and unpolarized nucleons (HERMES, COMPASS and STAR).

Ones again one needs to pay a tribute to the scientific intuition of N.N.Bogoliubov, initiated about 25 years ago a participation of JINR physicists in such important investigations. With the forthcoming discoveries in this field this initiative will be even more valuable.

REFERENCES


1. **Voss R.** — UFN, 1996, v.166, No.9, p.927-942.
2. **Savin I.** — In: Proc. of the SPIN 98 Symp., Protvino, Russia, edited by N.E.Tyurin et al., World Scientific, p.78-94.
3. **HERMES Collaboration, Ihseen H.** — Nucl. Phys. Proc. Suppl., 1999, v.74, p.133-137.
4. STAR Conceptual Design Report. BNL, Pub-5347, 1992.
5. COMPASS Proposal. CERN/SPSLC 96-14, 1996.
6. **Bogolubov N.N., Struminsky D.V., Tavkhelidze A.N.** — JINR Communication D-1968, Dubna, 1965.
7. See, for example, **Roberts R.G.** — Structure of the Proton: Deep Inelastic Scattering. Cambridge University Press, 1990.
8. Review of Particle Physics — Eur. Phys. J., 1998, v.C3 p.195-199.
9. **Krivokhizhin V.G. et al.** — Z. Phys., 1987, v.C36 p.51.
10. **Savin I.A.** — In Proc. of XXII Int. Conf. on High En. Phys., Leipzig, edit. by A.Meyer and E.Wieczorek, Zeuthen, 1984, v.II, p.251.
11. **Anselmino M., Efremov A., Leader E.** — Phys. Rep., 1995, v.261, p.1-124.
12. **Savin I.A., Smirnov G.I.** — Sov. J. of Part and Nucl., 1991, v.22, No.5, p.489; BCDMS: **Benvenuti A. et al.** — Z. Phys., 1994, v.C63. p.29.
13. **Arneodo M.** — Phys. Rep., 1994, v.240, p.301.
14. **Smirnov G.I.** — Eur. Phys. J., 1999, v.C10, p.239-247.